



# EXPERIMENTAL AND NUMERICAL STRESS ANALYSIS OF INVOLUTE SPLINED SHAFT

**Dr. Majid H. Faidh-Allah**  
Mechanical Engineering

**Zainab Amjed Abdul Khalik**

University of Baghdad

## ABSTRACT

In this study, the induced splined shaft teeth contact and bending stresses have been investigated numerically using finite element method (Ansys package version 11.0) with changing the most effecting design parameter, (pressure angle, teeth number, fillet radius and normal module), for internal and external splined shaft. Experimental work has been achieved using two dimensional photoelastic techniques to get the contact and bending stresses; the used material is Bakelite sheet type "PSM-4".

The results of numerical stress analysis indicate that, the increasing of the pressure angle and fillet radius decrease the bending stress and increase the contact stress for both internal and external spline shaft teeth while the increasing of the normal module and teeth number decrease the contact and bending stresses.

**Keywords:** Spline shaft, Finite Element Analysis, photoelastic

.(PSM.4)

## 1. INTRODUCTION

A Spline is a geometric feature used to join one shaft to another. It transmits torsion, but permits axial sliding. splined connections are widely used as a coupling mechanism in rotating machinery.

Splined shafts transmit torque from one rotating member to another at the same value and direction.

Splines are essentially stubby gear teeth formed on the outside of the shaft and on the inside of the hub of the load-transmitting component. Splines are generally much more expensive to manufacture than keys and are usually not necessary for simple torque transmission. They are typically used to transfer high torques [Shigley, 2008]. [D. A. Baker, 1999] calculated the maximum Von Mises stress for solid finite element models of splined shafts with straight-sided teeth for two types of spline shaft, stepped and partially spline shaft. Finite element analyses are performed for the cases of a stepped shaft of three different step size ratios ( $d/D$ ). The second set of models consists of a solid cylindrical shaft with incomplete spline teeth. The incomplete regions of the spline teeth are

(11) ANSYS

)

(

modeled in three radii (R). Bending, torsion, and combined loads are applied to each model, including several combinations of bending and torsion between pure bending and pure torsion. The stresses in the stepped splined shafts are up to 50% greater than nominal stresses in the non-splined section and up to 88% greater than nominal stresses splined section. Stresses in the partially splined shaft are up to 42% greater than the well developed nominal stress in the non-splined section of the shaft, and up to 7% greater than the nominal stresses in the splined section. [H. Yoshitake, 1962] presented an experimental investigation about the spline shaft by the three - dimensional photoelastic method and it is found that: The stress distribution of the spline shaft was measured, and the stress concentration factor was obtained. The results were coincident fairly well with those of other methods. The accuracy of the wedge method was checked and its value was about 5%. The stress distribution of the meshing spline shaft was investigated, and it was found that the maximum bending stress of the tooth was comparable with the maximum torsional stress. [A. Tjernberg, 2001] presented finite element model of a spline coupling between a shaft and a sleeve. The stress concentration factor is calculated and compared to analytical calculations. The pitch error caused by the irregular spacing between the spline teeth has been measured. The measurement of pitch error has been made of splines manufactured using two different milling methods. A simplified model has been created to calculate the approximate load on each tooth and the relative life. Induction hardened shafts with splines manufactured with one type of milling method have been fatigue tested. The calculations have showed that the life of a spline with pitch error is only 1/3-1/2 of the life of a spline with ideal pitching. [D. C. H. Yang and SH. H. Tong, 2007] studied the profile design of splines and keys components. The influence of spline profiles on the performance of power transmission is investigated. They presented the optimal design of spline profiles for three different design criteria. The method of calculus of variation is used to determine profile functions for maximum value. Analytical results are successfully obtained. They show that the splines with involute profiles lead to uniform deformation on the hub; in addition they can carry the maximum transmission load capacity. On the other hand, radial straight profiles result in optimum transmission efficiency

## 2.Numerical Stress Analysis of Spline Shaft Teeth:

Finite element analysis is a numerical method in which a particular body is subdivided into discrete partitions (called elements) that are bound by nodes. Each element is connected to adjacent elements by the nodes. The finite element method requires that the fundamental differential equations governing the overall problem be reduced to a system of algebraic equations from which a general solution is obtained. Boundary conditions and environmental factors are applied to the subdivided model. The equations governing the individual elements are then combined and solved to obtain the solution for the overall problem.

### 2.1 Convergence Test:

To ensure the accurate results of stress calculations, the element type must be chosen carefully, which is used to mesh the splined teeth models, so that the convergence test must be done at first and as follow:

1. Building up the internal and external spline models according to mathematical model.
2. Specifying the material properties as a structural, linear, elastic, isotropic with  $\nu = 0.3$ ,  $E = 200,000 \text{ N/mm}^2$ .
3. Specifying the applied load and boundary conditions (they are the same through the convergence test).

Specifying the element type as solid and using the following element type successively (anasio 64, Tetrahedrol 10 node 187, 8 node 185, 20 solid 186, 20 solid 95, Brick 8 node 45 and 10 node 92) with changing the coarser to each element in order to investigate the right element number as well the element type. The result of the convergence test show that the best element type that can be employed to mesh the model is 8 nodes 185 with 19964 elements with 29081 nodes as in Fig.1, Fig. 2 represents one external tooth meshed with these elements.

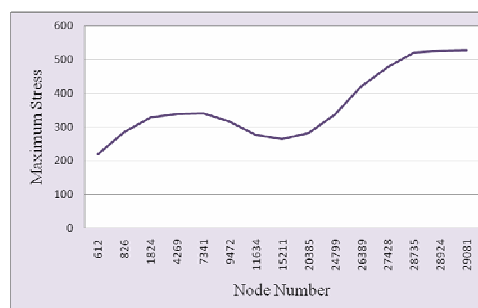
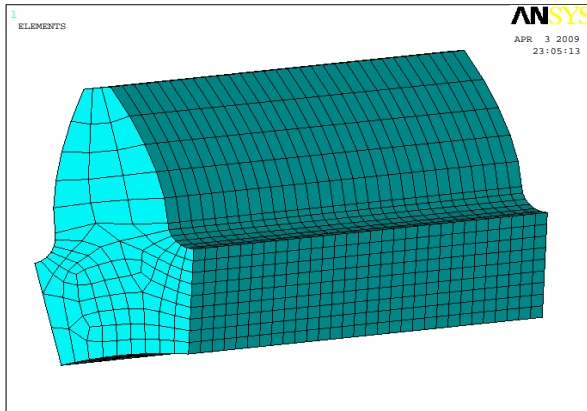


Fig. 1 Convergence test



**Fig. 2** One external tooth meshed with solid element 8 nodes

## 2.2 Development of Finite Element Models:

The development for finite element models is accomplished as follows [Jill Tombasco, 2004], [H. Tea Cong, 1996] and [Vera Nikolic, 2003].

1. Tooth surface equations of external and internal splines and portions of corresponding rim are considered for determination of the volumes of the designed bodies.
2. The proposed approach does not require an assumption on the load distribution in the contact area.
3. F. E. models of one tooth are applied.
4. Setting of boundary conditions is accomplished automatically.

The following ideas are considered:

- Node on the two sides and bottom part of the portion of the external rim are considered as fixed.
- Nodes on the two sides and bottom of the portion of the internal rim are considered as a rigid body.
- Input torque can be expressed as the sum of the applied nodal forces at radius of shaft ( $r_i$ ), thus

$$T = \sum_{i=1}^n F_i r_i \quad (1)$$

Where (T) is the input torque load, (n) is the total number of constrained nodes and ( $F_i$ ) is the tangential nodal force (usually  $F_i = F$ , is a constant value).

The boundary conditions can be seen in **Fig.3**

5. The contact algorithm of (FEA) computer program requires definition of contacting surfaces [Jamesn F. Doyle, 2004]. To define a contact pair completely, contact

and target elements, have to be referred to the same characteristic parameters.

6. The selected contact algorithm was Penalty method. The penalty method uses a contact “Spring” to establish a relationship between the two contact surfaces.

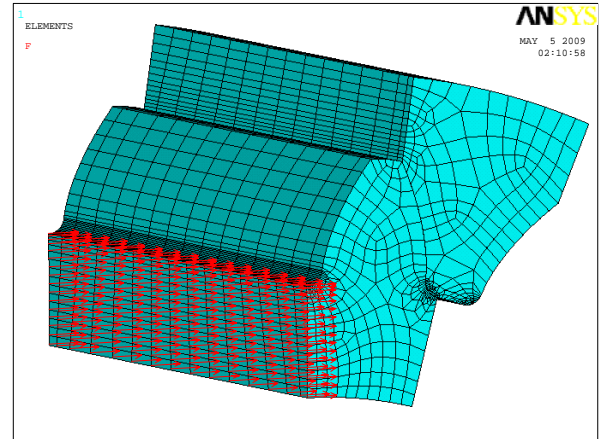


**Fig. 3** Boundary conditions for external and internal involute splines

## 3. Experimental Stress Analysis of Spline Shaft Teeth

Photoelastic stress analysis (photoelasticity) is a well known technique to perform stress analysis experimentally with many economic benefits to engineering design. Photoelastic, which provides both quantitative and qualitative analysis, allows a loaded model to be analyzed while still in the design stages, which means a design can be adjusted before production. A non- destructive technique, photoelasticity allows the same model to reuse during analysis. The universality of this method provides for its application to all areas of engineering design [U. Burgtorf, P. Dietz and M. Garzke, 1998].

In present photoelastic study the three-dimensional problem was reduced to a series of two- dimensional problem by calculation the stresses at a number of thin cross sections along the tooth length [R. Errichello,1978], it is sufficient to analyze only one slice of two-dimensional to determine the contact and bending stresses.

### 3.1 Photoelastic Method of Stress Analysis:

The birefringent material has been used to construct the transparent spline shaft models, internal and external splines. The basic equation that calculates experimentally the induced stresses is:

$$(\sigma_1 - \sigma_2) = n f / h \quad (2)$$

Where (n) represent the number of fringes, (v) is the material fringe constant and  $(\sigma_1 - \sigma_2)$  is

the difference in the principle stresses, (h) represent the tooth width, Eq. (2) can be arranged as:

$$f = \frac{(\sigma_1 - \sigma_2)}{n} h \quad (3)$$

Thus in a simple loading procedure for which a known principal stress difference can be easily expressed in terms of the applied load we can determine the fringe constant [D. L. Hitt, 2003].

### 3.2 Photoelastic Material and Photoelastic Model:

Used a transparent flat model made of a plastic material that is doubly refracting under stress such as Bakelite sheet type “PSM-4” with (6mm) thickness. This photoelastic material can be employed for two and three-dimensional studies. **Table1** shows the material properties determined from calibration test of specimen which has been cut from same material of sheet used to fabricate the tooth model. The segment model of one tooth profile has been made carefully to matching the output of the theoretical design. The spline teeth model was made 5 times the actual size, See **Fig.4**.The dimension of spline shaft geometry of the chosen profile are given in **Table 2**.

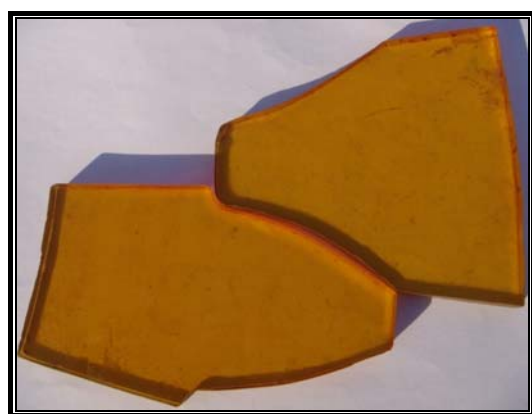


**Fig. 4** Spline Shaft Photoelastic Models

**Table 1** Mechanical Properties of Photoelastic Material

| Modulus of elasticity<br>N/mm <sup>2</sup> | Elastic limit<br>N/mm <sup>2</sup> | Poisson's ratio |
|--|------------------------------------|-----------------|
| 2.335714 e+003                             | 1.692 e+003                        | 0.4             |

**Table 2** Dimensions of Splined Shaft Mode

| Normal module (mm) | Normal pressure angle (Deg) | No. of teeth | Face Width (mm) |
|--------------------|-----------------------------|--------------|-----------------|
| 6                  | 30                          | 20           | 6               |

### 3.3 Experimental Apparatus and Experimental Procedure:

In the present photoelastic analysis, the splined teeth model was positioned in the loading fixture such that the area of contact on the external tooth profile matched the area of contact on the internal tooth profile. The external tooth model was firmly clamped to prevent rotation during applying load, and connected to the load sensor which was connected to the load cell to read the applied load. While the internal tooth model was connected to an arm connects to the crank handle to apply load by turning the load crank on the loading fixture.

Both a light and dark field was employed to increase the accuracy of the account of the fringes. Once load was established, the light and dark field photographs were taken of the fringe pattern in the spline model.

Before conducting any test on the model, the calibration of load cell must be checked. The model is then aligned in the field of the polariscope and the load is gradually applied to the models. **Fig. 5** shows the details of apparatus used in experimental analysis

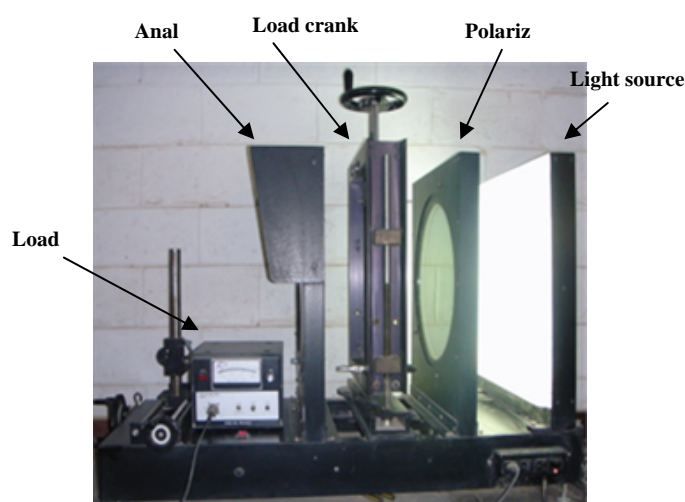


**Fig.5** Experimental Apparatus

### 4. Transition from Model to Prototype:



For many practical two dimensional elastic problems with forces applied to external boundaries, the stress depends upon geometry and external forces only [F. James Doyle and James W .Phillips, 1982].

The profile of the model is made geometrically similar to that of the prototype to be studied but not of the same size, and the applied load must be similarly distributed, but they may differ in magnitude by a factor of proportionality. Any stress ( $\sigma_p$ ) in the prototype can be determined from the corresponding stress ( $\sigma_m$ ) at the corresponding point in the model. The bending stress for the mating teeth can be calculated as follow [E. J. Hearn, 1977].

$$\sigma_b = (M y) / I \quad (4)$$

Where ( $\sigma_b$ ) is the bending stress, ( $M$ ) is the moment, ( $y$ ) is the half of width of the tooth and ( $I$ ) is the moment of inertia. The relation between the model and the prototype for bending stresses is:

$$\sigma_{bp} / \sigma_{bm} = ((M y) / I_p) / ((M y) / I_m) \quad (5)$$

Where all dimensions of model are five times the prototype dimensions and that leads to:

$$\sigma_{bp} = 25 \left( \frac{F_p}{F_m} \right) \sigma_{bm} \quad (6)$$

Table 1 shows the values of ( $E$  and  $\nu$ ) for models. The prototype properties are  $E=200,000 \text{ MN/m}^2$  and  $\nu = 0.3$ .

## 5. Results and Discussions:

The results of teeth stress analysis obtained experimentally by using photoelastic analysis and numerically by using Finite Element Analysis, (Ansys package), Version 11.0, are investigated.

In the numerical F.E.A several models have been analyzed with different cases of design of splined shaft such as pressure angle, normal modules, fillet radius and number of teeth and their effects on contact and bending stresses have been stated. Photoelastic study was performed to check the numerical analysis by determined values of contact and bending stress.

Form finite element (ANSYS) results, the variation of maximum contact and bending stresses with pressure angle, normal modules, fillet radius and number of teeth are plotted in Fig. (6) -- (13). The results showed that the increasing of the normal pressure angle decreases the bending stress and increase the contact stress

due to decrease the horizontal teeth load component, increasing the teeth number and normal module decrease the shared load (the applied load on each meshed tooth) and cause decreasing in both contact and bending stress and the increasing of the fillet radius decrease the bending stress due to the decreasing of stress concentration factor while that cause an increasing in the contact stress. At last it is important to notice that the internal spline shaft are in general have more resistance to the bending stresses than the external spline shaft and the cause of that is they have larger cross section area at the root region than the mating spline.

Fig.14 shows the photographs of photoelastic analysis that gives the maximum contact and bending stresses which were calculated from the analysis of photographs of the fringes. The comparison between experimental and numerical stress analyses for contact and bending stresses at load case (1) and load case (2) are given in Tables 3, 4, 5 and 6.

In case (1), the percentage errors of the maximum contact stress between two results are 14.742% and 16.666% in external and internal spline teeth , respectively and the percentage errors of the maximum bending stress between two results are 6.166% and 4.388% in external and internal spline teeth, respectively.

In case (2), the percentage errors of the maximum contact stress between two results are 12.116% and 17.006% in external and internal spline teeth, respectively and the percentage errors of the maximum bending stress between two results are 4.509% and 5.685% in external and internal spline teeth, respectively.

There was a difference in results between experimental and finite element analyses because of the errors in profile during cutting process. That's all because:

1. In the cutting process, the errors in the profile will be produced and this produce problems in practical application which effect on the localized of bearing contact.
2. The fringe order at contact point is very high because of the localized contact load and, therefore, the fringe order exactly at the contact point can never be measured accurately.
3. There may be some error in the calculation of the material fringe constant.

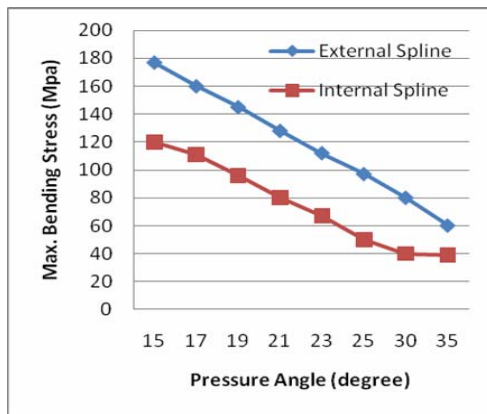


**Fig. (6)** Variation of bending stress for external and internal spline with pressure angle

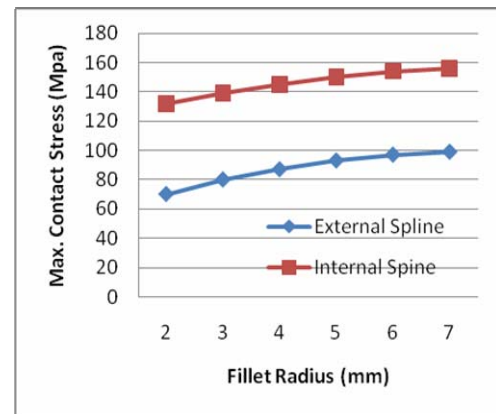


**Fig. (9)** Variation of bending stress for external and internal spline with pressure angle

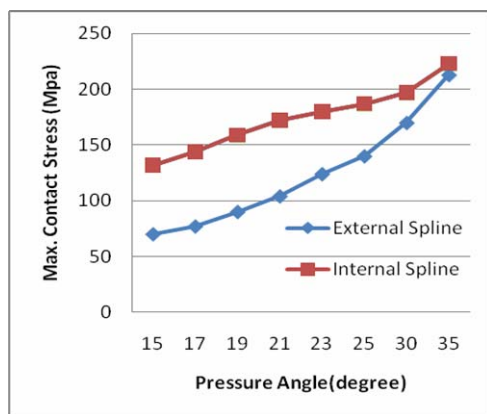


**Fig. (7)** Variation of bending stress for external and internal spline with pressure angle

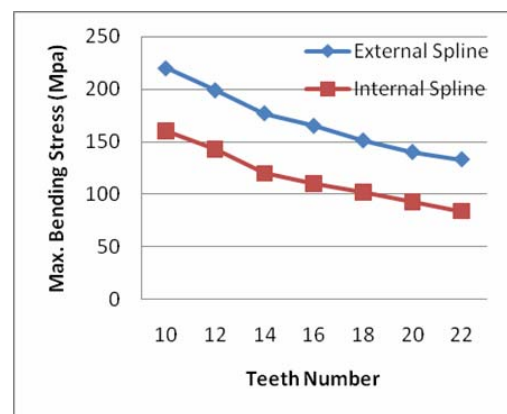


**Fig. (10)** Variation of bending stress for external and internal spline with pressure angle

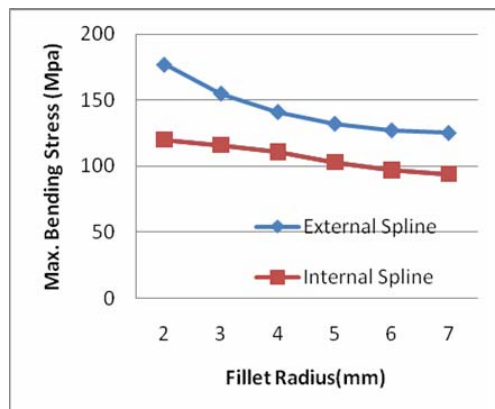


**Fig. (8)** Variation of bending stress for external and internal spline with pressure angle

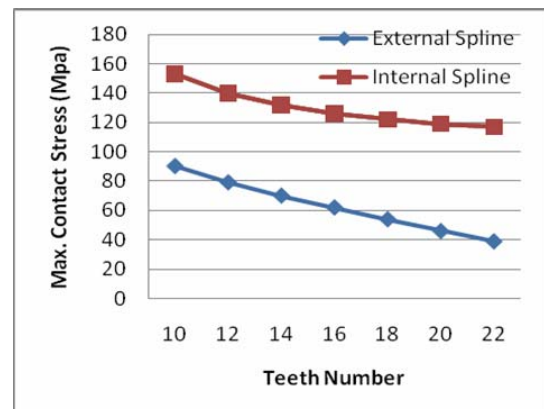


**Fig. (11)** Variation of bending stress for external and internal spline with pressure angle

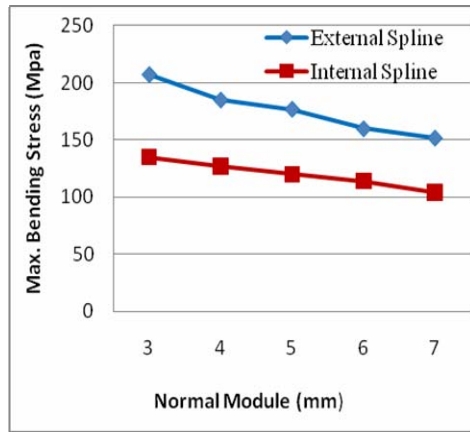


**Fig. (12)** Variation of bending stress for external and internal spline with pressure angle

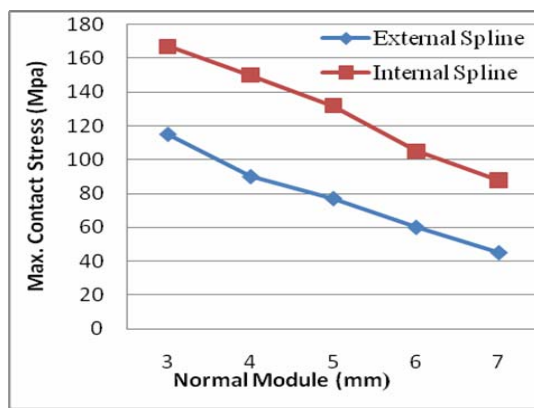


**Fig. (13)** Variation of bending stress for external and internal spline with pressure angle

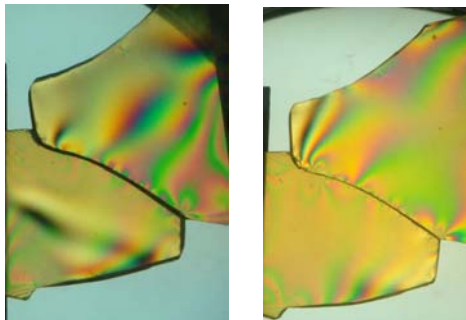


**Fig. 14** Results of photoelastic fringes show the contact and bending stresses for two load cases of spline teeth .

**Table 3** Comparison between experimental and numerical contact stress at load case (1)

| Maximum Contact Stress(Mpa) |              |           | Percentage Error (%) |
|-----------------------------|--------------|-----------|----------------------|
|                             | Experimental | Numerical |                      |
| External                    | 83.639       | 98.102    | 14.742               |
| Internal                    | 135.6        | 162.719   | 16.666               |

**Table 4** Comparison between experimental and numerical bending stress at load case (1)

| Maximum Bending Stress(Mpa) |              |           | Percentage Error (%) |
|-----------------------------|--------------|-----------|----------------------|
|                             | Experimental | Numerical |                      |
| External                    | 237.814      | 224       | -6.166               |
| Internal                    | 171.301      | 164.1     | -4.388               |

**Table 5** Comparison between experimental and numerical contact stress at load case (2)

| Maximum Contact Stress(Mpa) |              |           | Percentage Error (%) |
|-----------------------------|--------------|-----------|----------------------|
|                             | Experimental | Numerical |                      |
| External                    | 111.02       | 126.327   | 12.116               |
| Internal                    | 204.831      | 182.06    | -17.006              |

**Table 6** Comparison between experimental and numerical bending stress at load case (2)

| Maximum Bending Stress(Mpa) |              |           | Percentage Error (%) |
|-----------------------------|--------------|-----------|----------------------|
|                             | Experimental | Numerical |                      |
| External                    | 188.163      | 275.73    | -4.509               |
| Internal                    | 205.03       | 194       | -5.685               |

## 6. Conclusions:

The main conclusions obtained from the present work can be summarized as follow

1. In general the internal spline teeth offers a high resistance to the bending stress than the external spline teeth while they have a higher contact stresses than the external one so that the failure of the internal spline teeth occur at the flank region and at the fillet in the external spline teeth.
2. The increasing of the pressure angle and fillet radius reduce the induced fillet bending stress and increases the flank contact stress for both external and internal spline teeth.
3. Teeth number and normal module have a positive role one the performance of the spline shaft because of their substantial effect in the decreasing of the contact and bending stresses.
4. The bending stresses on the external teeth have the highest value comparable with bending stresses on internal teeth and contact stresses in internal and external teeth.

Automotive, control and robotic, Vol. 15, pages  
1055-1066, 2003

## REFERENCES

A.Tjernberg, "Load Distribution and Pitch Errors in a Spline Coupling". Journal of materials and design, No. 22, Pages 259-266, 2001.

D. A. Baker, "A Finite Element Study of Stresses in Stepped Splined Shafts, and Partially Splined Shaft under Bending, Torsion, and Combined Loadings". A thesis submitted in partial fulfillment of the requirements for the degree of Master of Science in Mechanical Engineering/ Virginia Polytechnic Institute and State University 1999.

D. C. H. Yang and SH. H. Tong, "On the Profile Design of Transmission Splines and Keys", Journal of Mechanism and Machine Theory, No.42, Pages 82-87, 2007.

D. L. Hitt, "Notes on Quantitative Photoelastic Analysis". ME124, 2003.

E. J. Hearn, "Mechanics of Materials". International series on material science and technology, VOL. 19, 1977.

F. James Doyle and James W. Phillips, "Manual on Experimental Stress Analysis". Fifth Edition, Society for Experimental Mechanics, 1982.

H. Tea Cong, "A Design Support System Gear Drive". Dep. Mech. Hanyang Univ., Korea, 1996.

H.Yoshitake,"Photoelastic Stress Analysis of the Spline Shaft". Japan society of Mechanical Engineers, Vol.5, No17, Pages195-201, 1962.

J. F. Doyle, "Modern Experimental Stress Analysis". Purdue University, Lafayette, USA, 2004.

J.Tombasco, "Photoelastic Dynamic Stress Analysis using Synchronized Strobe Techniques". Internet / Keywords: Photoelastic stress analysis, 2004.

R. Errichello, "Bending Stress in Gear Teeth Having Circular Arc Profiles- Part 2: Experimental Investigation". Transaction of the ASME, Journal of Mechanics Design, Vol.100, pages 395- 404, 1978.

Shigley, "Shigley's Mechanical Engineering Design". Eighth Edition, McGraw -Hill Companies, 2008.

U. Burgtorf, P. Dietz and M. Garzke, "Calculation of Involute Splines under Elastic Material Behaviour". International design conference, Germany, 1998.

V. Nikolic, "The Analysis of Contact Stress on Meshed Teeth's Flank Along the Path of Contact for a Tooth Pair". Series: Mechanics,

## NOMENCLATURES

### English symbols

| <u>Symbol</u> | <u>Description</u>                 | <u>Unit</u>       |
|---------------|------------------------------------|-------------------|
| E             | Modulus of elasticity              | MN/m <sup>2</sup> |
| $f$           | Material fringe constant           | N /mm             |
| $F_i$         | Nodal Force                        | N                 |
| h             | Thickness of the specimen          | mm                |
| I             | Moment of inertia                  | mm <sup>4</sup>   |
| M             | Moment                             | N.m               |
| $n$           | Number of fringes                  | ----              |
| n             | Node number subjected to force     | ----              |
| $r_i$         | Radius of Nodes Subjected to Force | Mm                |
| T             | Applied torque                     | N.m               |

### Greek symbols

| <u>mbol</u>               | <u>Description</u> | <u>Unit</u> |
|---------------------------|--------------------|-------------|
| $\nu$                     | Poisons ratio      | ----        |
| $\sigma_1$ and $\sigma_2$ | Principal stresses | Mpa         |
| $\sigma_b$                | Bending stress     | Mpa         |
| $\phi$                    | Pressure Angle     | degree      |